Cronin effect and high-$p_\perp$ suppression in d+Au collisions

D. E. Kahana[1] and S. H. Kahana[2]
[1]*31 Pembrook Dr., Stony Brook, New York 11790, USA*
[2]*Physics Department, Brookhaven National Laboratory Upton, New York 11973, USA*
(Received 3 September 2004; published 18 August 2005)

Great interest has attached to recent d+Au, $\sqrt{s} = 200A$ GeV data at RHIC, obtained with the BRAHMS detector. Between pseudorapidities $\eta = 0$ and $\eta = 3.2$ the appropriately defined ratio R[dAu/pp], comparing transverse-momentum spectra of d+Au to pp, exhibits a steady decrease with η. This diminution is examined within a two-stage simulation. In the first stage, initial nucleon-nucleon interactions are treated in parallel, as if occurring simultaneously, whereas the second stage is a considerably reduced energy hadronic cascade. This approach is by no means a standard hadronic cascade, never entailing an overly high density of cascading particles. Indeed a condition is imposed on the total multiplicity at the outset of the second stage permitting no overlap of intermediate interacting prehadrons. The result is an adequate description of the data, including the so-called Cronin effect. Additionally there is, in the second stage, clear evidence for suppression of relatively high transverse momentum $\eta = 0$ leading mesons (i.e., the Cronin effect is appreciably muted by final state interactions).

DOI: 10.1103/PhysRevC.72.024903 PACS number(s): 25.75.Nq

I. INTRODUCTION

It is instructive to begin with a comparison of the minimum-bias experimental distribution $dN^{\rm ch}/d\eta$ for charged particles at $\sqrt{s} = 200A$ GeV and our eventual attempt to describe this. These are shown in Fig. 1 together with the equivalent pp measurement without any normalizing factors imposed. The data shown are from UA5 [1] and PHOBOS [2]. Clearly charged particle production in d+Au is considerably enhanced relative to pp; but for large η the d+Au spectrum asymptotically joins pp, both in the data and in our simulation. It is also evident the $\eta = 3.2$ point is appreciably suppressed relative to $\eta = 0$, for d+Au but not for pp. This suppression, which extends to both soft and hard collisions, is "geometric." For the more forward, more positive η the most dominant contribution is from collisions along a ring at the nucleus periphery, whereas for midrapidity the entire nuclear volume plays a role. It will become clear that these pseudorapidity spectra, which are in fact integrals of the double differential cross sections $(1/2\pi p_\perp)[d^2N^{\rm ch}/dp_\perp\, d\eta]$, are dominated by quite small transverse momenta $p_\perp$. We examine this self-evident thesis in more detail as we proceed.

The BRAHMS collaboration [3] has focused on the η and $p_\perp$ dependence of the ratio

$$R[d{\rm Au}/pp] = \left(\frac{1}{N_{\rm coll}}\right)\frac{[d^2N^{\rm ch}/dp_\perp\, d\eta]\ (d{\rm Au})}{[d^2N^{\rm ch}/dp_\perp\, d\eta]\ (pp)}, \quad (1)$$

where $N_{\rm coll}$ is a calculated number of binary NN collisions occurring in minimum-bias d+Au. They consider also the combined η and $p_\perp$ dependence for varying centralities $c_{1,2}$ of

$$R_{c_i p} = \left[\frac{R_{c_i}(d{\rm Au}/pp)}{R_p(d{\rm Au}/pp)}\right], \quad (2)$$

where the denominator is the same ratio for a peripheral setting. The behavior of the former ratio we contend is determined mainly by the geometric-driven dynamics, which applies to both low and high transverse momentum, and by the $p_\perp$ distribution in pp collisions, for us an input to the nucleus-nucleus simulation. There are important dynamic modifications (e.g., the Cronin effect [4]), but the relation between low and high $p_\perp$ is to a large extent similar to that in pp. The observed behavior of $R_{c_i p}$ with pseudorapidity and centrality is determined by the asymptotic approach of $dN/d\eta$ in d+Au to that in pp at increasing η and the resulting diminished variation with η.

The code LUCIFER, developed for high-energy heavy-ion collisions has previously been applied to both SPS energies $\sqrt{s} = (17.2, 20)A$ GeV [5] and to RHIC energies $\sqrt{s} = (56, 130, 200)A$ GeV [6,7]. We present a brief description of the dynamics of this Monte Carlo simulation. Many other simulations of heavy-ion collisions exist and these are frequently hybrid in nature, using say string models in the initial state [8–15] together with final-state hadronic collisions, whereas some codes are purely partonic [16–20] in nature. Our approach is closest in spirit to that of RQMD and K. Gallmeister, C. Greiner, and Z. Xu as well as work by W. Cassing [8,21,22]. Certainly our results seem to parallel those of the latter authors.

The purpose of describing such high-energy collisions without introducing the evident parton nature of hadrons, at least for soft processes, was to set a baseline for judging whether deviations from the simulation measured in experiments existed and could then signal interesting phenomena. The division between soft and hard processes, the latter being in principle described by perturbative quantum chromodynamics (QCD), is not necessarily easy to identify in heavy-ion data. For the relatively simple d+Au system we are interested in separating the effects of our second stage, a lower energy hadronic cascade, from those of our first stage, a parallel rather than sequential treatment of initial (target)-(projectile) NN interactions.

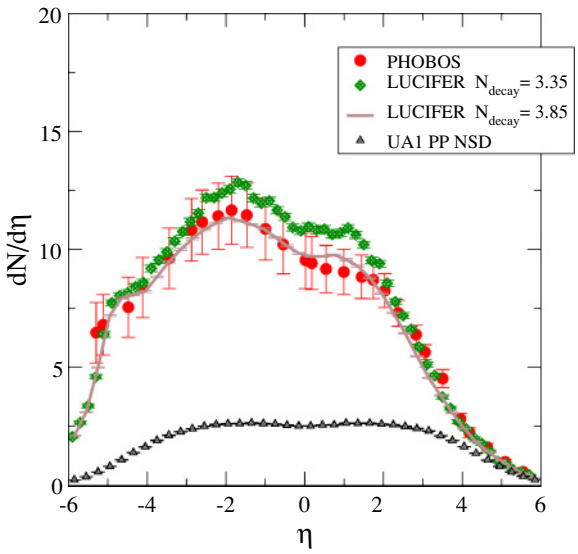

FIG. 1. (Color online) d+Au 200A GeV charged-hadron pseudorapidity spectra: Direct comparison of PHOBOS minimum bias data with LUCIFER simulations, the latter for $b \leqslant 16$ fm. Two calculations are shown, slightly differently normalized, one for which the average prehadron decays into 3.35 observed mesons and one for which this number is 3.8. Both are somewhat above that expected for pure NN production, indicating some calculated events exceed the multiplicity constraint discussed in the text. The absence of collision number divisors is instructive, revealing both the considerable production of final state mesons at $\eta = 0$, in excess of pp, and the apparent asymptotic approach of both data and calculation to pp at the largest observed η.

II. THE SIMULATION

A. Stage I

The first stage I of LUCIFER considers the initial interactions between the separate nucleons in the colliding ions A+B, but is not a cascade. The totality of events involving each projectile particle happen essentially together or one might say in parallel. Neither energy loss nor creation of transverse momentum ($p_\perp$) are permitted in stage I, clearly an approximation. A model of NN collisions [5,6], incorporating most known inclusive cross section and multiplicity data, guides stage I and sets up the initial conditions for stage II. The two-body model, clearly an input to our simulation, is fitted to the elastic, single diffractive (SD) and nonsingle diffractive (NSD) aspects [23] of high-energy pp collisions [1,24] and $p\bar{p}$ data [25]. It is precisely the energy dependence of the cross sections and multiplicities of the NN input that led to our successful prediction [2,6] of the rather small (13%) increase in $dN^{\rm ch}/d\eta$ between $\sqrt{s} = 130$ and $\sqrt{s} = 200A$ GeV, seen in the PHOBOS data [26].

A history of the collisions that occur between nucleons as they move along straight lines in stage I is recorded and later used to guide determination of multiplicity. Collision-scaled random walk in transverse momentum fixes the $p_\perp$ to be ascribed to the baryons at the start of stage II. The overall multiplicity, however, is subject to a modification, based, as we believe, on natural physical requirements [6].

If a sufficiently hard process, for example, Drell-Yan production of a lepton pair at large mass occurred, it would lead to a prompt energy loss in stage I. Hard quarks and gluons could similarly be entered into the particle lists and their parallel progression followed. This has not yet been done. One viewpoint and justification for our approach is to say we attempt to ignore the direct effect of color on the dynamics, projecting out all states of the combined system possessing color. In such a situation there should be a duality between quark-gluon or hadronic treatments.

The collective/parallel method of treating many NN collisions between the target and projectile is achieved by defining a group structure for interacting baryons. This is best illustrated by considering a prototype proton-nucleus (p+A) collision. A group is defined by spatial contiguity. A proton at some impact parameter $b(\bar{x}_\perp)$ is imagined to collide with a corresponding "row" of nucleons sufficiently close in the transverse direction to the straight line path of the proton (i.e., within a distance corresponding to the NN cross section). In a nucleus-nucleus (A+B) collision this procedure is generalized by making two passes: on the first pass one includes all nucleons from the target that come within the given transverse distance of some initial projectile nucleon, and then on the second pass one includes, for each target nucleon so chosen, all of those nucleons from the projectile approaching it within the same transverse distance. This totality of mutually colliding nucleons, at more or less equal transverse displacements, constitute a group. The procedure partitions target and projectile nucleons into a set of disjoint interacting groups as well as a set of noninteracting spectators in a manner depending on the overall geometry of the A+B collision. Clearly the largest groups in p+A will, in this way, be formed for small impact parameters b; whereas for the most peripheral collisions the groups will almost always consist of only one colliding NN pair. Similar conclusions hold in the case of A+B collisions.

In stage II of the cascade we treat the entities that rescatter as prehadrons. These prehadrons, both baryonic or mesonic in type, are not the physical hadron resonances or stable particles appearing in the particle data tables, which materialize after hadronization. Importantly, prehadrons are allowed to interact starting at early times, after a short production time [27], nominally the target-projectile crossing time $T_{AB} \sim R_{AB}/\gamma$. The mesonic prehadrons are imagined to have ($q\bar{q}$) quark content and their interactions are akin to the dipole interactions included in models relying more closely on explicit QCD [27,28], but are treated here as colorless objects.

Some theoretical evidence for the existence of comparable colorless structures is given by Shuryak and Zahed [29] and by certain lattice gauge studies [30]. In these latter works a basis is established for the persistence of loosely bound or resonant hadrons above the QCD critical temperature T_c to $T \sim (1.5 - 2.0) \times T_c$. This implies a persistence to much higher transverse energy densities $\rho(E) \sim (1.5 - 2.0)^4 \rho_c$, hence to the early stages of a RHIC collision. Accordingly we have incorporated into stage II *hadron-sized* cross sections for the interactions of these prehadrons, although early on it may in fact be difficult to distinguish their color content.

Such larger cross sections indeed appear to be necessary for the explanation of the apparently large elliptical flow parameter found in measurements [31,32].

The prehadrons, which when mesonic may consist of a spatially close, loosely correlated quark-antiquark pair, are given a mass spectrum between m_π and 1 GeV, with correspondingly higher upper and lower limits allowed for prehadrons, including strange quarks. The Monte Carlo selection of masses is governed by a Gaussian distribution,

$$P(m) = \exp[-(m - m_0)^2/w^2], \tag{3}$$

with m_0 a selected center for the prehadron mass distribution and $w = m_0/4$ the width. The nonstrange mesonic mass center is set at $m_0 \sim 600$ MeV, and for strange at $m_0 \sim 750$ MeV. Small changes in m_0 and w have little effect because the code is constrained to fit hadron-hadron data.

Too high an upper limit for m_0 would destroy the soft nature expected for most prehadron interactions when they finally decay into "stable" mesons. The same proviso is in place for prebaryons that are restricted to a mass spectrum from m_N to 2 GeV. However, in the present calculations the prebaryons are for simplicity taken just to be the normal baryons. The mesonic prehadrons have isospin structure corresponding to ρ, ω, or K^*, whereas the baryons range across the octet and decuplet.

Creating these intermediate degrees of freedom at the end of stage I simply allows the original nucleons to distribute their initial energy momentum across a larger basis of states or Fock space, just as is done in string models or, for that matter, in partonic cascade models. Eventually, of course, these intermediate objects decay into physical hadrons and for that purpose we assign a uniform decay width $\sim\Gamma_f$, which then plays the role of a hadronization or formation time.

B. Groups

Energy loss and multiplicity in each group of nucleons is estimated from the straight line collision history. To repeat, transverse momentum of prebaryons is assigned by a random walk having a number of steps equal to the number of collisions suffered. The multiplicity of mesonic prehadrons cannot be similarly directly estimated from the number of *NN* collisions in a group. We argue [5,6] that only spatial densities of generic prehadrons below some maximum are allowable, viz. the prehadrons must not overlap spatially [33] at the beginning of stage II of the cascade. The KNO-scaled multiplicity distributions, present in our *NN* modeling, are sufficiently long tailed that imposing such a restriction on overall multiplicity can affect results even in p+A or d+A systems. In earlier work [5,7] the centrality dependence of $dN/d\eta$ distributions for RHIC energy Au+Au collisions was well described with such a density limitation on the prehadrons. Incidentally, the mesonic prehadrons in more massive ion-ion collisions are formed at high density, virtually touching, and certainly strongly interacting. It might be therefore appropriate to refer to such a condensed medium in say a Au+Au system as a liquid.

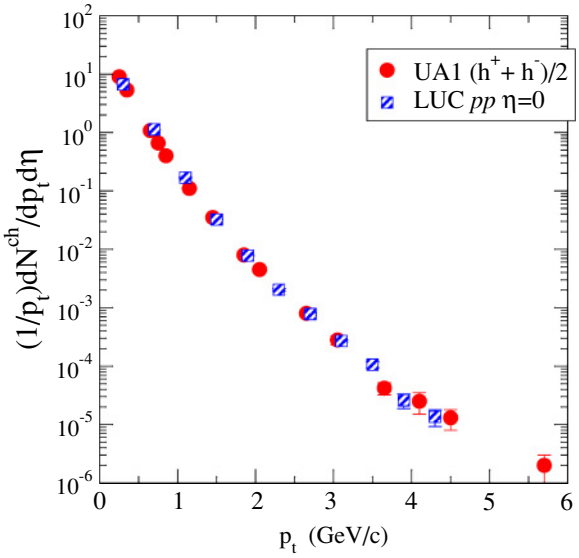

FIG. 2. (Color online) 200 GeV transverse-momentum spectra: UA1 vs LUCIFER. The LUCIFER fit to the UA1 *NN* data [24] provides a basic input for both low- and high-$p_\perp$ for nucleus-nucleus simulations.

Importantly, the cross sections in prehadronic collisions were assumed to be the same size as hadronic (e.g., meson-baryon or meson-meson), at the same center of mass energy, thus introducing no additional free parameters into the model. Where the latter cross sections or their energy dependences are inadequately known we employed straightforward quark counting to estimate the scale. In both SPS Pb+Pb and RHIC Au+Au events at several energies it was sufficient to impose this constraint at a single energy. The inherent energy dependence in the KNO-scaled multiplicities of the *NN* inputs and the geometry then take over.

C. High Transverse Momenta

One question that has yet to be addressed concerns the high $p_\perp$ tails included in our calculations. In principle, LUCIFER is applicable to soft processes (i.e., at low transverse momentum). Where the cutoff in $p_\perp$ occurs is not readily apparent. In any case we can include high-$p_\perp$ meson events through their presence in the basic hadron-hadron interaction, which is of course an input rather than a result of our simulation. Thus in Fig. 2 we display the NSD $(1/2\pi p_\perp)(d^2N^{\text{charged}}/dp_\perp\, d\eta)$ from UA1 [24]. One can use a single exponential together with a power-law tail in $p_\perp$, or alternatively two exponentials, to achieve a fit of the output in pp to UA1 $\sqrt{s} = 200$ GeV data. A sampling function of the form

$$f = p_\perp[a\exp(-p_\perp/w) + b/(1 + (P_\perp/\alpha)^\beta)], \tag{4}$$

gives a satisfactory fit to the pp data in the Monte Carlo.

This pp $p_\perp$ spectrum, inserted into the code, is then applied to the meson $p_\perp$ distribution in d+Au. No correction is made for possible energy loss in stage I, an assumption parallel to that made by the BRAHMS and all other RHIC experiments, in analyzing $p_\perp$ spectra and multiplicities irrespective of low

or high values. Because we impose energy-momentum conservation in each group, a high-$p_\perp$ particle having, say, several GeV/c of transverse momentum, must be accompanied in the opposite transverse direction by one or several compensating mesons. Such high-$p_\perp$ particles are not exactly jets to the extent that they did not originate in our simulation from hard parton-parton collisions, but they yield the same observable experimental behavior.

That the high $p_\perp$ prehadrons produced should be given hadron-like cross sections perhaps requires some justification. We offer two possibilities. Molnar [31] has tried to correct the "flow" deficiencies of partonic cascades by introducing coalescence of quarklike partons at an early stage in the cascade. Clearly such coalescence probabilities will decrease steeply with increasing transverse momentum, at say small rapidity, but that is just what is observed in the meson production from both pp and AA. We then argue that the coalescence probability will be greatest for the larger transverse-sized mesons produced.

Furthermore, and actually relevant to our specific simulation, the earliest meson-meson collisions in our second stage cascade II (described below) have a first peak in time at some 0.15–0.25 fm/c but in fact appreciable collision and decay extend to considerably later time. This permits even smaller prehadrons to have appreciably increased their transverse size before collision and simultaneously suggests most collisions are between comovers. Also, the premesons, which dominate the second stage dynamics, are given only 4/9 the total cross section of baryon-baryon and hence need only possess considerably reduced effective tranverse sizes than say baryons.

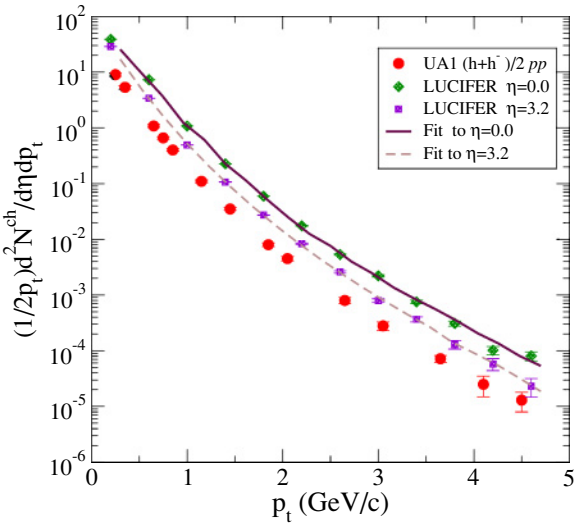

FIG. 3. (Color online) The simulated minimum bias charged transverse-momenta spectra for d+Au at $\eta = (0, 3.2)$ are placed alongside the UA1 data. Fits to these LUCIFER simulations, used to interpolate the simulation, are also shown. The latter fits use a combination of a single exponential at low $p_\perp$ and a power law at higher values.

D. Initial Conditions for stage II

The final operation in stage I is to set the initial conditions for the hadronic cascade in stage II. The energy momentum taken from the initial baryons and shared among the produced prehadrons is established and an upper limit placed on the production multiplicity of prehadrons and normal hadrons. A final accounting of energy sharing is carried out through an overall four-momentum conservation requirement. We emphasize that this is carried out separately within each group of interacting nucleons.

The spatial positioning of the particles at this time could be accomplished in a variety of ways. We have chosen to place the prehadrons in each group inside a cylinder, initially having the longitudinal size of the nucleus for a p+A collision and having the longitudinal size of the interaction region at time T_{AB} in an A+B collision, then allowing the cylinder to evolve freely according to the longitudinal momentum distributions, for a fixed time τ_f, defined in the rest frame of each group. At the end of τ_f the multiplicity of the prehadrons is limited so that if given normal hadronic sizes $\sim(4\pi/3)(0.6)^3$ fm^3, they do not overlap within the cylinder. The transverse geometry of the interaction region is reproduced at each impact parameter.

Up to this point longitudinal boost invariance is completely preserved, because stage I is carried out using straight line paths. The technique of defining the evolution time in the group rest frame is essential to minimizing the residual frame dependence that inevitably arises in any cascade, hadronic or partonic, when transverse momentum is considered because the finite size of the colliding objects implied by their nonzero interaction cross sections.

III. STAGE II: FINAL-STATE CASCADE

Stage II is as stated a straightforward cascade in which the prehadronic resonances interact and decay as do any normal hadrons present or produced during this cascade. Appreciable energy having being finally transferred to the produced particles, these "final state" interactions occur at considerably lower energy than the initial nucleon-nucleon collisions of stage I. As pointed out, during stage II the interaction and decay of both prehadrons and hadrons is allowed. In the case of d+Au, although less abundant than with a more massive projectile, these final state interactions are, as we will see, still of some relevance.

We are then in a position to present results for d+Au collisions. These appear in Fig. 1, as previously referred to, and Figs. (2–6), some of which are comparisons with the measurements of both BRAHMS and PHOBOS [2,3]. In fact the plot of experimental data in Fig. 1 is from PHOBOS [2]. This PHOBOS reference also exhibits comparisons with several theoretical calculations [9,34–36]. Two of these references [35,36] describe much of the measured η distribution at negative η near the target, whereas one [36] apparently accounts for the extreme backward tail; this is a subject to which we will return.

The initial conditions created to start the final cascade could have perhaps been arrived at through more traditional, perhaps

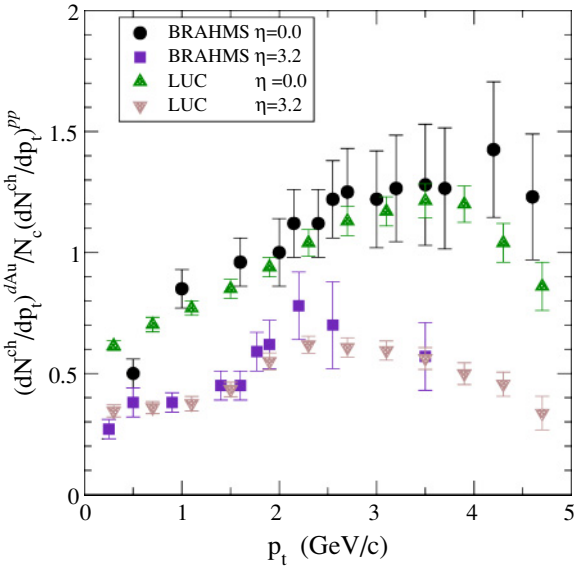

FIG. 4. (Color online) Minimum-bias R[dAu/pp] for $\eta = (0, 3.2)$: The BRAHMS results are compared to the collision-number-normalized calculations. The latter are obtained using the results in Fig. 3 with $N_{\rm coll} = 7.0$, compared to the BRAHMS choice 7.2 ± 0.3. The presence of a Cronin effect in the simulation is evident, with, however, a flatter $p_\perp$ dependence obtaining for the larger η. As in the BRAHMS analysis the ratio R[dAu/pp] for $\eta = 3.2$ is given for negatively charged hadrons (h^-) only. The theoretical ratio for $\eta = 3.2$ is likely more accurate than either the pp or dAu calculations separately.

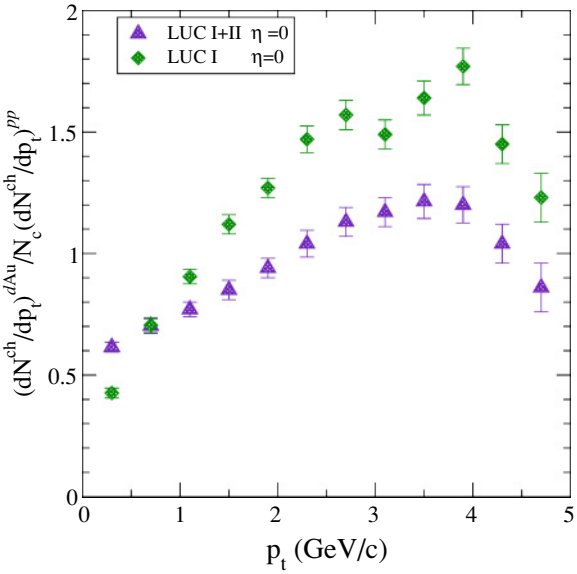

FIG. 5. (Color online) Effect of the final-state hadronic cascade: Cronin effect for stage I vs, I+II. The latter, II, of course is the lower energy hadronic cascade. The Cronin enhancement of minimum bias $d^2N/d\eta dp_\perp$ for $\eta = 0$ is markedly reduced by the second stage of LUCIFER. For larger $p_\perp$ one might refer to this phenomenon as final-state "jet" suppression. The diminution is muted for larger η. For more massive ion-ion collisions one can expect a considerably greater reduction.

partonic, means. The second stage would then still proceed as it does here. We reiterate that our purpose has been to understand to what extent the results seen in Figs. (1–6) are affected by stages I and II separately (i.e., do they arise from initial or from final-state interactions).

IV. RESULTS: COMPARISON WITH DATA

Figure 3 contains the simulated charged transverse-momenta spectra for d+Au at $\eta = (0, 3.2)$ alongside the UA1 data. The many orders of magnitude fall in transverse-momentum yields with $p_\perp$ is apparent. Aside from low $p_\perp$ the d+Au curves for increasing $p_\perp$ appear roughly parallel to pp; small but interesting deviations show up when the ratios previously defined are displayed. Additionally, direct integration of the spectra indicates that $\geqslant 90\%$ of the charged rapidity densities result from $p_\perp \leqslant 0.7$ GeV/c. Having built in no energy loss effects on these $p_\perp$ distributions in the initial state, so that a similar falloff obtaining in both d+Au and pp is all but preordained, the overall ratio between $\eta = 0.0$ and $\eta = 3.2$ seems to be driven completely by low-$p_\perp$ physics. In fact the multiplicity choice at given pseudorapidity and transverse momentum is only mildly influenced by $p_\perp$ dependence aside from that already present in the pp input.

In Fig. 4 the calculated LUCIFER ratios $R[d\text{Au}/pp]$ are plotted alongside those for BRAHMS [3] at both $\eta = 0$ and $\eta = 3.2$. The theoretical results are obtained using $N_{\rm coll} = 7.0$ rather than the value closer to 7.2 employed by BRAHMS. Our calculation of the average number of collisions in

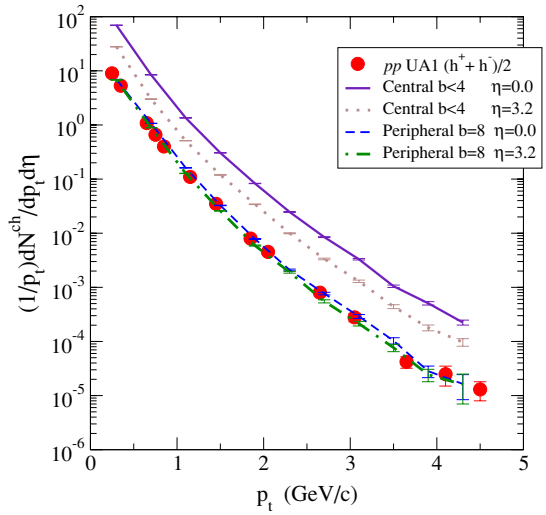

FIG. 6. (Color online) Centrality dependence of R[dAu/pp]. The two sets of $\eta = (0, 3.2)$ transverse-momentum distributions for one central $b \leqslant 4.0$ fm and one more peripheral impact parameter $b = 8.0$ fm are displayed against the UA1 pp data. Evidently the η dependence is strong for the central choice and virtually vanishing for the more peripheral collision, with the latter distributions closely matching UA1. Indeed if one proceeds to sufficiently large η R[dAu/pp], as presently defined, it will become flat and achieve the value $1/N_{\rm coll}$.

minimum-bias d+Au, defined as $b \leqslant 16$ fm, is approximately 7.0. The Cronin affect is evident in the calculated $\eta = 0$ spectrum, less so for $\eta = 3.2$. This is not unexpected.

A. Jet Suppression

A very interesting result is obtained by turning off the final cascade (i.e., stage II). Then the prehadrons produced in stage I evolve or decay into stable particles after the time $\tau_f \sim 1/(\Gamma)$ and do not otherwise suffer interaction. This situation is described in Fig. 5, where it is clear that the magnitude of the Cronin enhancement of $dN/dp_\perp$ is considerably magnified. The Cronin effect is then very much a creature of I (i.e., a product of the transverse momentum gained in collisions with nucleons in the target). The nucleons suffering the largest number of virtual collisions in I, through random walk, receive the highest $p_\perp$ as do the mesonic hadrons to which they give rise. Incidentally, Fig. 5 also indicates that a compensating increase in transverse-momentum density occurs at the lowest $p_\perp$ when stage II, the final cascade, is present (i.e., momentum lost at high $p_\perp$ is transferred by collision to particles with lower $p_\perp$).

One might well turn this around and declare that the final state scattering of a given prehadron with comovers has cut down the Cronin effect, a reduction that suggests the applicability of the term *jet suppression* by final-state interactions. The change in the $p_\perp$ spectrum is considerably less for $\eta \sim 3$, where Fig. 1 indicates considerately less comovers are present, and indeed the Cronin enhancement is in any case less evident at the more forward η.

The spillover of such stage II comovers decreases with increasing separation from the target pseudorapidities and the ratio $R[d\text{Au}/pp]$ is flatter as a function of $p_\perp$. This is, again, easily understandable: the most peripheral collisions involving the least number of participants will contribute more strongly to more forward rapidities. Both the unrenormalized theoretical and measured d+Au $dN/d\eta$ curves appear to merge with pp at the largest pseudorapidities, as shown in Fig. 1. One expects to see a corresponding behavior with decreasing centrality and decreasing participant nucleon number.

B. Centrality dependence of R[*d*Au/*pp*]

A similar theme then is repeated in Fig. 6 where the $p_\perp$ spectra for two quite different degrees of centrality differ markedly; the disparate centralities are defined by $b \leqslant 4$ fm and $b = 8$ fm. The η dependence exhibited for $b = 8$ fm, a clearly peripheral geometry, is very muted with both $\eta = 0$ and $\eta = 3.2$ showing a strong resemblance to the pp $\eta = 0$ data. The more central choice, $b \leqslant 4$, is subject to additional strong pseudorapidity variation. This explains at least qualitatively, the behavior of the second ratio BRAHMS focuses on (i.e., R_{cp} [3]). The crossover of this ratio with centrality as a function of η is explained by the flatter dependence in η discussed here. The differing number N_{coll} then must be invoked to complete the picture but it plays only a passive role, the alteration of the $p_\perp$ distribution already evident in Fig. 6 for widely differing centralities or impact parameter plays the essential role.

V. CONCLUSIONS

It is hard to conclude definitively from what is presented here that the gluon saturation [34,37] and attendant color-glass-condensate interpretation [34,38] of the BRAHMS data is not a more fundamental explanation of the measurements discussed here. Certainly the low-x basis for this modeling is related to the increasing η picture presented here, and perhaps the gluon saturation aspect of that approach is mirrored in, and underpins, the prehadron multiplicity limitation employed above.

It would seem, however, that the direct attempt at a pQCD explanation of this behavior must claim that, at the very least, all soft mesons are produced in essentially hard collisions. The presentation here provides an interesting case for relying on the dynamics of soft, low-$p_\perp$, processes, essentially mirrored in hard processes, to produce the major features of the BRAHMS data. True enough, the high-$p_\perp$ tails in distributions are merely tacked on in our approach, but legitimately so by using the pp data as input to the nucleus-nucleus cascade. The pp $dN/dp_\perp$ distribution to a large extent drives the variation with $p_\perp$ seen in d+Au, altering only slightly the hard η-dependent ratio from the soft. One only need add the assumption that the $p_\perp$ tails in d+Au do not exhibit any drastic nonmonotonic behavior.

The nascent appearance of appreciable high-$p_\perp$ suppression, especially for $\eta = 0$ (Fig. 5), suggests that enhanced suppression will occur in a full Au+Au collision. Whether the complete, or an appreciable fraction of, jet suppression seen in RHIC experiments can be explained by final-state interactions remains to be established. We note that C. Greiner and coauthors [21] and Cassing [22] have commented forcefully on precisely this point, also in a hadron-based cascade setting.

We indicated we would return to the target pseudorapidity region. It is of direct relevance to do this for discussion of specifics in d+Au but also for the implications for Au+Au and other complex systems. For the deuteron projectile PHOBOS data not only extend further backward than other experiments or calculations but also exhibit a feature, perhaps a shoulder, near where our calculations exhibit a peak in the charged baryons (see Fig. 1). It would clearly be of some import to have particle identification in the present measurements of η and $p_\perp$ distributions. Considering the d+Au system, one notes that transverse momentum distributions near the target, or further back in η, are significantly softer, again possibly anticipating high-$p_\perp$ suppression to be associated with the symmetric massive ion collisions.

ACKNOWLEDGMENTS

Useful discussion with the BRAHMS, PHENIX, PHOBOS, and STAR collaborations are gratefully acknowledged, especially with C. Chasman, R. Debbe, and F. Videbaek. This manuscript has been authored under the U.S. DOE grant DE-AC02-98CH10886. One of the authors (SHK) is also grateful to the Alexander von Humboldt Foundation (Bonn, Germany) and the Max-Planck Institute for Nuclear Physics (Heidelberg) for continued support and hospitality.

[1] G. Ekspong (UA5 Collaboration), Nucl. Phys. **A461**, 145c (1987); G. J. Alner (UA5 Collaboration), Nucl. Phys. **B291**, 445 (1987).

[2] B. B. Back *et al*. (PHOBOS Collaboration), Phys. Rev. Lett. **91**, 072302-1 (2003); B. B. Back *et al*. (PHOBOS Collaboration), nucl-ex/0311009, Nov. 2003.

[3] I. Arsene *et al*. (BRAHMS Collaboration), nucl-ex/0307003; I. Arsene *et al*. (BRAHMS Collaboration), nucl-ex/0403050; I. Arsene *et al*. (BRAHMS Collaboration), submitted to Phys. Rev. Lett., nucl-ex/0307003; I. Arsene *et al*. (BRAHMS Collaboration), Phys. Rev. Lett. **93**, 242303 (2004).

[4] J. W. Cronin *et al*., Phys. Rev. D **11**, 3105 (1975).

[5] D. E. Kahana and S. H. Kahana, *Proceedings, RHIC Summer Study'96*, 175–192, BNL, Upton, N.Y. July 8–19, 1996; Phys. Rev. C **58**, 3574 (1998); **59**, 1651 (1999).

[6] D. E. Kahana and S. H. Kahana, Phys. Rev. C **63**, 031901(R) (2001).

[7] D. E. Kahana and S. H. Kahana, *Proc. International Conference on the Physics of the Quark-Gluon Plasma, Ecole Polytechnique, Palaiseau,* France, Sept. 4–7, 2001; D. E. Kahana and S. H. Kahana, nucl-th/0208063.

[8] H. Stoecker and W. Greiner, Phys. Rep. **137**, 277 (1986); R. Matiello, A. Jahns, H. Sorge, and W. Greiner, Phys. Rev. Lett. **74**, 2180 (1995).

[9] H. Sorge, Phys. Rev. C **52**, 3291 (1995).

[10] S. A. Bass *et al*., Nucl. Phys. **A661**, 205 (1999).

[11] B. Andersson, G. Gustafson, G. Ingleman, and T. Sjostrand, Phys. Rep. **97**, 31 (1983); B. Andersson, G. Gustafson, and B. Nilsson-Almqvist, Nucl. Phys. **B281**, 289 (1987).

[12] A. Capella and J. Tran Van, Phys. Lett. **B93**, 146 (1980); Nucl. Phys. **A461**, 501c (1987); A. Capella, *et al*., Eur. Phys. J. C **40**, 129 (2005); hep-ph/0403081.

[13] K. Werner, Z. Phys. C **42**, 85 (1989); K. Werner and J. Aichelin, Phys. Rev. Lett. **76**, 1027 (1996); H. J. Drescher, M. Hladik, S. Ostapchenko, and K. Werner, *Proceedings of the "Workshop on Nuclear Matter in Different Phases and Transitions,"* Les Houches, France, March 31–April 10, 1998; K. Werner, Invited lecture, given at the Pan-American Advanced Study Institute "New States of Matter in Hadronic Interactions" Campos de Jordao, Brazil, January 7–18, 2002, hep-ph/0206111.

[14] B. Zhang, C. M. Ko, B.-A. Li, and Z. W. Lin, nucl-th/9904075; Z. W. Lin and C. M. Ko, Phys. Rev. C **68**, 054904 (2003); Z. W. Lin *et al*., Nucl. Phys. **A698**, 375 (2002).

[15] J. Ranft and S. Ritter, Z. Phys. C **27**, 413 (1985); J. Ranft, Nucl. Phys. **A498**, 111c (1989).

[16] D. H. Boal, *Proceedings of the RHIC Workshop I (1985)*; Phys. Rev. C **33**, R2206 (1986).

[17] K. J. Eskola, K. Kajantie, and J. Lindfors, Nucl. Phys. **B323**, 37 (1989).

[18] X.-N. Wang and M. Gyulassy, Phys. Rev. D **44**, 3501 (1991); X.-N. Wang, nucl-th/000814 and nucl-th/0405029; hep-ph/0405125.

[19] K. Geiger and B. Mueller, Nucl. Phys. **B369**, 600 (1992); K. Geiger, Phys. Rev. D **46**, 4965 (1992); **46**, 4986 (1992); *Proceedings of Quark Matter'83*; Nucl. Phys. **A418**, 257c (1984); Phys. Rev. D **51**, 3669 (1995).

[20] S. A. Bass, B. Mueller, and D. K. Srivastava, Phys. Lett. **B551**, 277 (2003); S. A. Bass *et al*., Nucl. Phys. **A661**, 205 (1999).

[21] K. Gallmeister, C. Greiner, and Z. Xu, Phys. Rev. C **67**, 044905 (2003).

[22] W. Cassing, K. Gallmeister, C. Greiner, Nucl. Phys. **A735**, 277 (2004); J. Geiss, C. Greiner, E. Bratkovskaya, and U. Mosel, Phys. Lett. **B447**, 31 (1999).

[23] K. Goulianos, Phys. Rep. **101**, 169 (1983).

[24] C. Albajar *et al*. (UA1 Collaboration), Nucl. Phys. **B335**, 261 (1990).

[25] Y. Eisenberg *et al*., Nucl. Phys. **A461**, 145c (1987); G. J. Alner *et al*., *ibid*. **B291**, 445 (1987); F. Abe *et al*., Phys. Rev. D **41**, 2330 (1990).

[26] B. B. Back *et al*. (PHOBOS Collaboration), Phys. Rev. Lett. **88**, 22302 (2002).

[27] B. Z. Kopeliovich *et al*., Nucl. Phys. **A740**, 211 (2004).

[28] A. H. Mueller, Eur. Phys. J. A **1**, 19 (1998).

[29] E. V. Shuryak and I. Zahed, Phys. Rev. D **69**, 046005 (2004); Phys. Rev. C **70**, 021901 (2004).

[30] S. Datta, F. Karsch, P. Petreczky, and I. Wetzorke, hep-lat/0208012; J. Phys. G **30**, S1347 (2004); hep-lat/0309012.

[31] D. Molnar and M. Gyulassy, nucl-th/0102031; nucl-th/0104018; D. Molnar, Talk presented at workshop on "Creation and Flow of Baryons in Hadronic and Nuclear Collisions," ECT, Trento, Italy, May 3–7, 2004 (unpublished).

[32] S. S. Adler *et al*. (PHENIX Collaboration), Phys. Rev. Lett. **91**, 182301 (2003); C. Adler *et al*. (STAR Collaboration), Phys. Rev. Lett. **87**, 182301 (2001); S. Manly (PHOBOS Collaboration), *Proceedings of the 20th Winter workshop on Nuclear Dynamics*, Trelawney Beach, Jamaica, March 15–20, 2003.

[33] K. Gottfried, Phys. Rev. Lett. **32**, 957 (1974); Acta. Phys. Pol. B **3**, 769 (1972).

[34] L. McLerran and R. Venugopalan, Phys. Rev. D **49**, 3352 (1994); **59**, 094002 (1999); D. Kharzeev, E. Levin, and L. McLerran, Phys. Lett. **B561**, 93 (2003).

[35] M. Gyulassy and X. N. Wang, Comput. Phys. Commun. **83**, 307 (1994).

[36] Z. W. Lin and C. M. Ko, Phys. Rev. C **68**, 054904 (2003).

[37] L. V. Gribov, E. M. Levin, and M. G. Ryskin, Phys. Rep. **100**, 1 (1983); Nucl. Phys. **B188**, 555 (1981); A. H. Mueller and J. Qiu, *ibid*. **B268**, 427 (1986); E. M. Levin and M. G. Ryskin, Phys. Rep. **189**, 267 (1990).

[38] D. Kharzeev, E. M. Levin, and L. McLerran, Phys. Lett. **B561**, 93 (2003); L. McLerran, hep-ph/0402137 (2004); D. Kharzeev, E. M. Levin, and L. McLerran, Nucl. Phys. **A748**, 627 (2005); hep-ph/0403271 (2004).